

# Magnetotransport Properties of Ultrathin LaMnO<sub>3</sub> Layers

Oleg SHAPOVAL, Alexander BELENCHUK, Efim ZASAVITSKY, Valeriu KANTSER,  
IEN, AS RM, str. Academiei 3/3, MD 2028, Chisinau, Republica Moldova  
shapoval@lises.asm.md  
Vasily MOSHNYAGA

Erstes Physikalisches Institut, Universität Göttingen, Friedrich-Hund-Platz 1, 37077 Göttingen,  
Germany

**Abstract** – We report the transport and magnetic properties of La-deficient ultrathin films of La<sub>1-x</sub>MnO<sub>3</sub> (LMO) grown on SrTiO<sub>3</sub> (STO) and engineered by using different interfacial layers. LMO layer and adjusting interface oxide (LaO-STO and SMO) layers were grown by a metalorganic aerosol deposition technique with monolayer accuracy. The role of LaO-TiO<sub>2</sub> interface in the formation of ferromagnetic metallic state in very thin LMO films was demonstrated. Ferromagnetic metallic ground state in LMO films with the thickness down to 6 monolayers is stabilized by a combination of a La-deficiency and the interface-induced doping.

**Index Terms** – magnetotransport, metal-insulator transition, metalorganic aerosol deposition, oxide interfaces, thin film.

## I. INTRODUCTION

To enhance the functionality of all-oxide based devices the idea of the interface engineering of multilayered oxide heterostructures was put forward in the last few years. LaMnO<sub>3</sub> (LMO) is one of the promising materials used for the interfacial design of different multilayer systems. The stoichiometric LMO with the nominal  $t_{2g}^3 e_g^1$  occupancy of Mn<sup>3+</sup> ions is an insulator with strong Mott-Hubbard correlations in a half-filled  $e_g$  band [1]. An A-type antiferromagnetic (AFM) ground state originates due to the orbital ordering of  $e_g$ -orbitals with ferromagnetic (FM) in-plane and AFM out-of-plane exchange interactions. Nevertheless, LMO can be easily transformed into an FM metal, particularly in thin films [2] and superlattices of LMO/SMO [3] and LMO/STO [4]. The ferromagnetism was shown to be due to the change of: a) stoichiometric cationic composition; b) optimal oxygen content as well as c) due to epitaxial stabilization of a nonstoichiometric state in the layers grown on SrTiO<sub>3</sub> (STO) (100) substrates [2, 5]. The “electron leakage” phenomenon, caused by the polar discontinuity at the interfaces, was shown to control the magnetotransport in superlattices [4, 6]. The main parameter, influencing the direction of charge leakage and, therefore, the magnetic properties, is the substrate-induced epitaxial strain. The interest to LMO as a functional material was recently stirred up by the demonstration of a metal-insulator transition at  $T_{MI} > 400$  K in a heavy La-deficient films [7].

An important question, concerning to electronic and structural reconstruction at the interfaces, is the atomic structure of stacking planes. The LMO/SMO system demonstrates exclusively the LaO-MnO<sub>2</sub>-SrO sequence of atomic planes at the interface [8]. In contrast, the LMO/STO system reveals two types of interfaces due to different A- and B-site occupancies in the perovskite lattices. Namely, 1) (LaO-MnO<sub>2</sub>)-(SrO-TiO<sub>2</sub>) (compactly MnO<sub>2</sub>-SrO) and 2) (MnO<sub>2</sub>-LaO)-(TiO<sub>2</sub>-SrO) (or LaO-TiO<sub>2</sub>) [9] interfaces were observed. In this case one should expect different interface-induced properties [10]. An example of such different properties attributed to A<sup>1</sup>O-B<sup>2</sup>O<sub>2</sub> and A<sup>2</sup>O-B<sup>1</sup>O<sub>2</sub> interfaces

for the A<sup>1</sup>B<sup>1</sup>O<sub>3</sub>-A<sup>2</sup>B<sup>2</sup>O<sub>3</sub> stacked perovskites was demonstrated for the well-known LaAlO<sub>3</sub>/SrTiO<sub>3</sub> system [11], where AlO<sub>2</sub>-LaO-TiO<sub>2</sub> stacked planes are electronically reconstructed and show a metallic behavior, whereas the AlO<sub>2</sub>-SrO-TiO<sub>2</sub> interface is insulating due to atomic reconstruction.

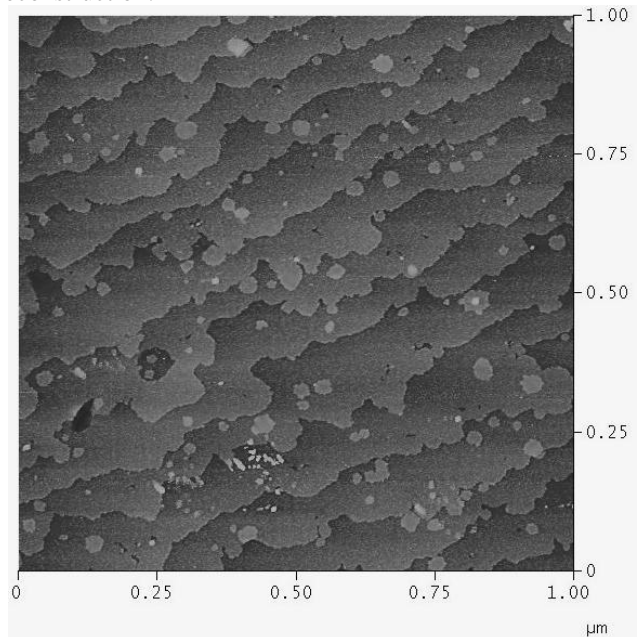


Fig. 1. STM image of 10 nm LMO layer deposited on TiO<sub>2</sub>-terminated surface of STO(100) substrate.

A single heterojunction for an A<sup>1</sup>B<sup>1</sup>O<sub>3</sub> layer, grown on the STO(100) substrate, can be modified by TiO<sub>2</sub>- or SrO-termination of the substrate surface. In the case of multilayered A<sup>1</sup>B<sup>1</sup>O<sub>3</sub>-A<sup>2</sup>B<sup>2</sup>O<sub>3</sub> structures a conventional growth techniques produce two types of interfaces [9]. The first layer starts from A<sup>1</sup>O-plane on TiO<sub>2</sub>-terminated surface STO(100) substrate and terminates by B<sup>1</sup>O<sub>2</sub>-plane; the next layer repeats the alternation of AO- and BO<sub>2</sub>-planes. A possibility to tailor the superlattices with single type of interface by introducing an extra-plane was recently demonstrated for LMO/STO system [4]. The presence of

extra LaO-planes in manganite layers and TiO<sub>2</sub>-planes in titanate layers was confirmed by STEM combined with EELS analysis.

The aim of the presented work was to study magnetotransport properties of ultrathin LMO films with thicknesses comparable to the thickness of single layers in SL's. To design the LMO-based layered structures with optimized FM metallic behavior two approaches were applied: 1) the La-deficiency was intentionally generated in the LMO layer and 2) ultrathin LMO films were engineered by different interfaces.

## II. EXPERIMENT AND RESULTES

The samples were prepared by a metalorganic aerosol deposition (MAD) technique, elaborated earlier for the preparation of complex oxide thin films and further developed for the deposition of ultrathin films and superlattices [12]. Aerosols of organic solutions, containing metal  $\beta$ -diketonates (e.g. La-, Sr-, Mn-acetylacetonates), were sprayed onto a heated substrate. A film grows on the substrate as a result of a heterogeneous pyrolysis reaction of the metalorganic component. Within the MAD technique one can easily manipulate the precursor solutions, which contain either a single precursor for mono-oxide layers or a mixture of two and more precursors to produce layers of complex oxides. The monolayer accuracy was achieved by accurate calibration of dosing units. Vacuum-free MAD technique allowed us to interrupt deposition process and to continue the preparation of the layered structure after intermediate express measurements.

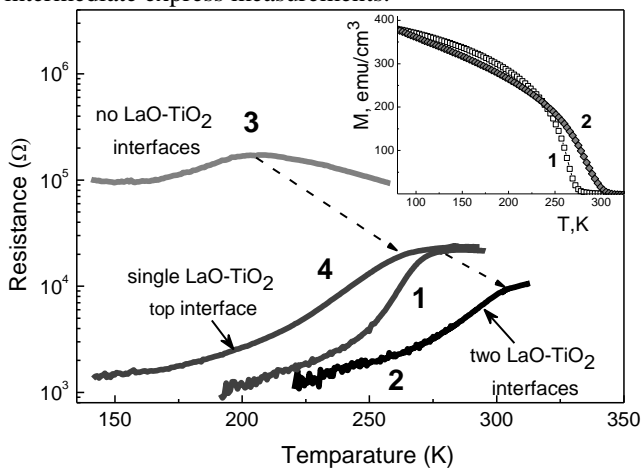


Fig. 2. Evolution of transport properties of 10 nm LMO layers deposited on STO(100) substrates and equipped with: (1) bottom LaO-TiO<sub>2</sub> interface; (2) top and bottom LaO-TiO<sub>2</sub> interfaces; (3) no LaO-TiO<sub>2</sub> interface; (4) top LaO-TiO<sub>2</sub> interface. Inset: Magnetization as function of temperature.

STO(100) substrate was chosen due to the possibility to study the influence of both surface terminations. The atomically smooth TiO<sub>2</sub>-terminated STO(100) with terrace steps of one unit cell in height was obtained by treating the crystal surface with a pH-controlled NH<sub>4</sub>F-HF solution [13]. SrO-terminated surface was produced by deposition of SrO monolayer (ML) on TiO<sub>2</sub>-terminated surface. The exact oxygen stoichiometry in the prepared LaMnO<sub>3</sub> layers was assumed due to a high (atmosphere) gas pressure conditions [12]. As the criteria of a stoichiometric La/Mn=1:1 relation we used the insulating behavior of the film, unique for a stoichiometric LMO, as well as smooth and flat surface morphology (Fig. 1) with terraces inherited from STO. The

deviation of La molar content from the “right” La/Mn-ratio in the solution was used in the sequel as a measure of the La-deficiency. The La-deficiency of LMO layers was varied in the range 0-12%. The thickness of LMO films was  $d=6-30$  unit cells (u.c.) or  $d=2.5-12$  nm.

LMO layers were deposited directly onto both TiO<sub>2</sub>- and SrO-terminated substrates or onto the STO surface, buffered by 2 u.c. of SMO. The top surface of LMO films have been remained free or covered by 2 u.c. of the cap layer, e.g. STO or SMO. Electron transport measurements were performed by standard 4-probe technique using commercial PPMS from “Quantum Design”. Magnetization was measured by means of commercial SQUID (MPMS, “Quantum Design”).

The role of LaO-TiO<sub>2</sub> interface was examined on series of samples with the same La-deficiency,  $\delta=6\%$ , and thickness of LMO layer. The influence of LaO-TiO<sub>2</sub> interfaces on the electron transport as a function of temperature is shown in Fig. 2. We suppose that the growth of LMO on the TiO<sub>2</sub>-terminated STO(100) from a solution, containing both La and Mn precursors, occurs in the following way. It starts from LaO-plane, forming the LaO-TiO<sub>2</sub> interface, and terminates with MnO<sub>2</sub> plane completing perovskite monolayer [9]. Thus, the LMO film with one (bottom) LaO-TiO<sub>2</sub> interface and free surface (top) was prepared after deposition of 26 perovskite unit cells of LMO. Such film demonstrates a metal-insulator (MI) transition at  $T_{MI}=285$ K and metallic behavior at low temperatures (curve 1 Fig. 2). A deposition of one monolayer of LaO, followed by 2 u.c. of STO on the top surface of the LMO film has resulted in the enhancement of  $T_{MI}$  by 45 K and in the decrease of the resistance at  $T_{MI}$  by 2 times (curve 2 Fig. 2). An LMO film without LaO-TiO<sub>2</sub> interfaces was prepared by the deposition of one monolayer of SrO onto the TiO<sub>2</sub>-terminated STO(100) prior to the deposition of LMO. In this case the manganite had to start the growth from the MnO<sub>2</sub> plane. LMO film with bottom SrO-MnO<sub>2</sub> interface and free top surface shows a decreased  $T_{MI}=210$ K and an insulating behavior at low temperatures (curve 3 Fig. 2). Deposition of 2 u.c. of STO on the top of LaO-terminated manganite film results in the formation of an LaO-TiO<sub>2</sub> top interface, thus, recovering the transport (curve 4 Fig. 2) to that described above for the film with one LaO-TiO<sub>2</sub> bottom interface.

We assume that optimized metallic behavior in LMO engineered films is because each LaO-TiO<sub>2</sub> interface creates effective conductive channels close to (or inside) the LMO layer. Magnetization as a function of temperature (see inset to Fig. 2) reveals, however, an unexpected behavior: after adding the second LaO-TiO<sub>2</sub> interface the Curie temperature ( $T_C$ ) was increased up to 305 K (the film with one interface shows  $T_C=275$  K). The increase of  $T_C$  correlates with increase of  $T_{MI}$ , but  $T_C$  is consistently lower than  $T_{MI}$ . Surprisingly, the saturation magnetization and magnetic hysteresis did not change after adding the second interface,  $M_s \sim 400$  emu/cm<sup>3</sup>  $\sim 2.5$   $\mu_B$ /Mn. This value is larger than that for undoped LMO [14] but it is significantly lower than magnetization for optimal doped manganites,  $M_s \sim 3.7$   $\mu_B$ /Mn [15]. Relatively high residual resistivity,  $\rho_{10K} = 1.6 \cdot 10^{-4}$   $\Omega$ cm, also indicates insufficient doping level.

Magnetic and transport properties of the samples with different thickness and the same La deficiency of LMO layers (see Fig. 3) stay in line with the probably lowered doping level. The highest temperature of the metal-insulator transition  $T_{MI} \sim 330$  K was achieved in LMO with the

thickness 26 uc and La-deficiency,  $\delta=6-8\%$ . The resistance shows metallic behavior down to the lowest temperature. By decreasing the thicknesses of LMO layer a decrease of  $T_{MI}$  and an increase of the resistance was observed. The thickness dependence of the transport properties can be rationalized within the “electron leakage” from the interface into the LMO layer. The reduced oxidation state in the sample is consistent with some degree of electron doping, coming from the electron from the extra (LaO) plane. The depth of charge spreading is larger than 2 uc as calculated for the insulating LMO [6]; it looks like charge is evenly distributed among the tens of LMO unit cells [4]. By reducing the thickness of LMO, one extra-electron distributed among smaller amount of LMO unit cells would give a stronger reduction of the averaged oxidation state. Such scenario suggests that LMO layers become progressively less hole-doped as the thickness is reduced, i.e. it is consistent with an increased electron leakage into LMO. Finally, for samples thinner than as 3 nm (6-7 uc) no metallic behavior was more observed regardless to the La deficiency; note that 2.5 nm thick film still remains ferromagnetic.

A further support for the above model comes from magnetization measurements. We observed a gradual decrease of  $M_S$  with decreasing of the LMO thickness (see Fig. 4a), that correlates both with the decrease of  $T_C$  and  $T_{MI}$ . Magnetic hysteresis behavior also comes to agreement with this model. The value of coercive field  $H_c \sim 30$  Oe indicates magnetic homogeneity of the 26 uc thick film. Apparently (see Fig. 4b)), magnetic inhomogeneity increases and the saturation magnetization decreases dramatically with decreasing of the thickness, i.e.  $M_S < 1 \mu_B/\text{Mn}$  for the 6 uc thick film, that is typical for an undoped LMO [14]. From a magnetic point of view only, the system looks like a weak ferromagnet. However, the  $e_g$ -hole is localized within a certain regions with very few Mn-ions. The ground state is a mixed state, composed from a disordered nm-size “double-exchange” metallic clusters and coexisting insulating domains. Even for high magnetic fields the system with magnetically aligned FM clusters do not reach the percolation limit [16] even if they grow in size.

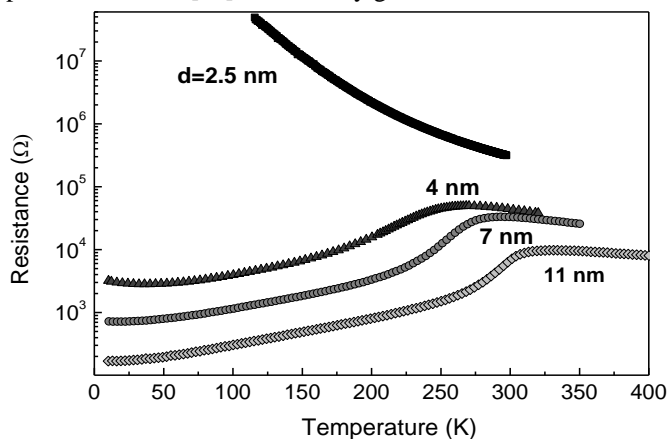


Fig. 3. Dependence of transport properties on temperature for STO-LMO-STO structures with different LMO layer thickness.

Inversion of the LaO-TiO<sub>2</sub> interface to SrO-MnO<sub>2</sub> by introducing SrO extra-layer (see Fig. 2) leads to the degradation of transport properties. A new design of SrO-

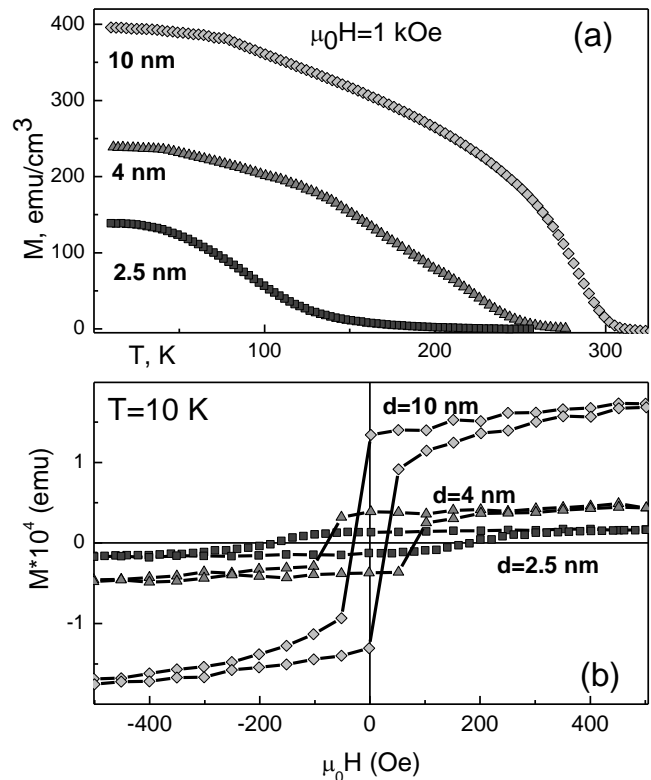


Fig. 4. Magnetization as a function of temperature (a) and magnetic hysteresis (b) for the STO-LMO-STO structures with different thickness of LMO layers.

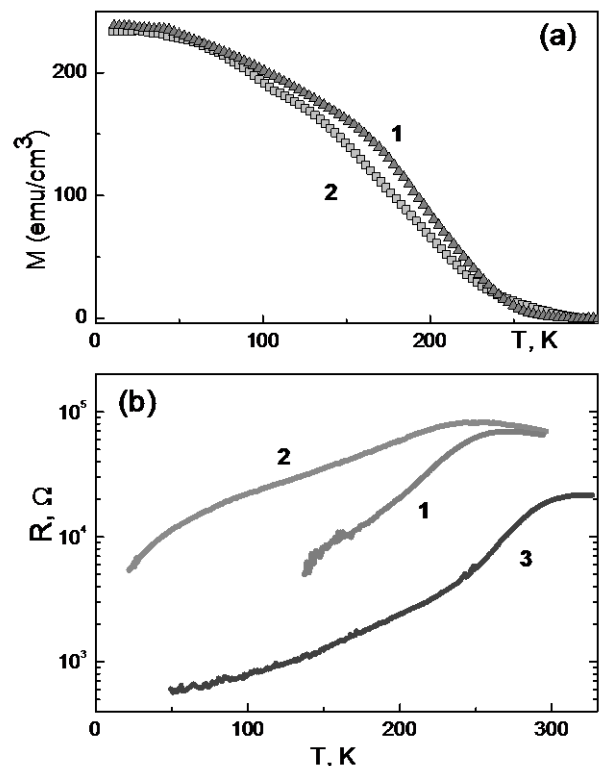


Fig. 5. Magnetization as a function of temperature (a) and resistance as a function of temperature (b) for: (1) STO-LMO(10 ML)-STO; (2) SMO-LMO(6 ML)-SMO; (3) SMO-LMO(10 ML)-SMO structures.

MnO<sub>2</sub> could improve the magnetotransport in LMO layer. According to the calculations [6] the Mn  $e_g$  electrons leak out from the LMO layer to the SMO one and change the magnetism at the interface, while away from the interface,

the magnetism of the respective bulk materials is preserved. Introduction of the 2 u.c. of SMO as the buffer and the capping layers allowed us to change the direction of the charge leakage and as a consequence to restore metallic behavior in very thin LMO films.

The resistance of SMO-LMO-SMO structure was found to be about 5 times lower than the resistance for STO-LMO-STO sample with the same thickness (10 u.c.) and La-deficiency (see Fig. 5(b)). LMO film confined by 2 SMO u.c. demonstrates metallic behavior down to the thickness of 6 u.c. The saturation magnetization and  $T_C$  of SMO-LMO(6 u.c.)-SMO and STO-LMO(10 u.c.)-STO are very similar (Fig. 5(a)), but the thinning of LMO layer in any way leads to rising of inhomogeneity that reflects in increased resistance (curve 2 in Fig. 5(b)). It is worth to note that the upper limit of the layer thickness is absent in the case of La-deficient LMO with ferromagnetic metallic behavior.

### CONCLUSIONS

We have shown that tailoring of the interfaces can be very effective in modifying the magnetotransport properties of ultrathin LMO films. Combination of the doping effects due to the La-deficiency with the interface-induced doping allowed us to preserve ferromagnetic metallic behavior in STO-LMO-STO structures with the thickness down to 10 u.c. of LMO. Interface modification of LMO layers by the 2 u.c. thick SMO bottom and top interfaces has led to a further shrinkage of the metallic LMO layer thickness down to 6 u.c. Engineering of the single type LaO-TiO<sub>2</sub> interface in the STO/LMO stacked perovskites can be performed within the MAD technique by deposition of an extra LaO plane. Thus, we show the possibility to change the natural growth sequence, i.e. AO-BO<sub>2</sub>, along the <100> direction of the perovskite structure.

### REFERENCES

- [1] A. Yamasaki, *et al.*, "Pressure-Induced Metal-Insulator Transition in LaMnO<sub>3</sub> Is Not of Mott-Hubbard Type," *Physical Review Letters*, vol. 96, p. 166401, 2006.
- [2] A. Gupta, *et al.*, "Growth and giant magnetoresistance properties of La-deficient La<sub>x</sub>MnO<sub>3-δ</sub> (0.67 < x < 1) films," *Applied Physics Letters*, vol. 67, pp. 3494-3496, 1995.
- [3] A. Bhattacharya, *et al.*, "Metal-Insulator Transition and Its Relation to Magnetic Structure in (LaMnO<sub>3</sub>)<sub>2n</sub>/(SrMnO<sub>3</sub>)<sub>n</sub> Superlattices," *Physical Review Letters*, vol. 100, p. 257203, 2008.
- [4] J. Garcia-Barriocanal, *et al.*, "'Charge Leakage" at LaMnO<sub>3</sub>/SrTiO<sub>3</sub> Interfaces," *Advanced Materials*, vol. 22, pp. 627-632, 2010.
- [5] P. Orgiani, *et al.*, "Enhanced transport properties in La<sub>x</sub>MnO<sub>3-δ</sub> thin films epitaxially grown on SrTiO<sub>3</sub> substrates: The profound impact of the oxygen content," *Applied Physics Letters*, vol. 95, pp. 013510-3, 2009.
- [6] B. R. K. Nanda and S. Satpathy, "Polar catastrophe, electron leakage, and magnetic ordering at the LaMnO<sub>3</sub>/SrMnO<sub>3</sub> interface," *Physical Review B*, vol. 81, p. 224408, 2010.
- [7] P. Orgiani, *et al.*, "Multiple double-exchange mechanism by Mn<sup>2+</sup> doping in manganite compounds," *Physical Review B*, vol. 82, p. 205122, 2010.
- [8] J. Verbeeck, *et al.*, "SrTiO<sub>3</sub>(100)/(LaMnO<sub>3</sub>)<sub>m</sub>(SrMnO<sub>3</sub>)<sub>n</sub> layered heterostructures: A combined EELS and TEM study," *Physical Review B*, vol. 66, p. 184426, 2002.
- [9] M. Varela, *et al.*, "Oxide Interfaces Under the Electron Microscope," *Microscopy and Microanalysis*, vol. 14, pp. 1346-1347, 2008.
- [10] H. Zenia, *et al.*, "Electronic and magnetic properties of the (001) surface of hole-doped manganites," *Physical Review B*, vol. 71, p. 024416, 2005.
- [11] D. H. A. B. J. Mannhart, H.Y. Hwang, A.J. Millis and J.-M. Triscone, "Two-Dimensional Electron Gases at Oxide Interfaces," *MRS Bulletin*, vol. 33, pp. 1027-1034, 2008.
- [12] K. Gehrke, *et al.*, "Interface controlled electronic variations in correlated heterostructures," *Physical Review B*, vol. 82, p. 113101, 2010.
- [13] M. Kawasaki, *et al.*, "Atomic Control of the SrTiO<sub>3</sub> Crystal Surface," *Science*, vol. 266, pp. 1540-1542, December 2, 1994 1994.
- [14] C. Adamo, *et al.*, "Electrical and magnetic properties of (SrMnO<sub>3</sub>)<sub>n</sub>/(LaMnO<sub>3</sub>)<sub>2n</sub> superlattices," *Applied Physics Letters*, vol. 92, pp. 112508-3, 2008.
- [15] J. M. D. Coey, *et al.*, "Mixed-valence manganites," *Advances in Physics*, vol. 48, pp. 167 - 293, 1999.
- [16] P. A. Algarabel, *et al.*, "Peculiar ferromagnetic insulator state in the low-hole-doped manganites," *Physical Review B*, vol. 67, p. 134402, 2003.